



## Abstract

Using a highly resolved atmospheric general circulation model the impact of different glacial boundary conditions on precipitation and atmospheric dynamics in the North Atlantic region is investigated. Seven 30-yr time slice experiments of the Last Glacial Maximum (21 ka ago) and of a less pronounced glacial state – the Middle Weichselian (65 ka ago) – are compared to analyse the sensitivity to changes in the ice sheet distribution, in the radiative forcing, and in the prescribed time-varying lower boundary conditions, which are taken from a lower-resolved but fully-coupled atmosphere-ocean general circulation model.

The strongest differences are found for simulations with different heights of the Laurentide ice sheet. A large altitude of this ice sheet leads to a southward displacement of the jet stream and the storm track in the North Atlantic region. These changes in the atmospheric dynamics generate a band of increased precipitation in the mid-latitudes across the Atlantic to southern Europe in winter, while the precipitation pattern in summer is only marginally affected. The impact of the radiative forcing differences between the two glacial periods and of the prescribed time-varying lower boundary conditions – evaluated using two simulations of the Last Glacial Maximum with a global mean temperature difference of  $1.1\text{ }^{\circ}\text{C}$  – are of second order compared to the one of the Laurentide ice sheet. They affect the atmospheric dynamics and precipitation in a similar but less pronounced manner as the topographic changes.

## 1 Introduction

During glacial periods the climate is fundamentally different compared to today. The understanding of the underlying processes, which are responsible for these differences, is of great interest. In this context the Last Glacial Maximum (LGM, 21 ka ago) is one of the most extensively studied glacial periods. Using a multi-proxy approach, sea surface temperatures (SSTs) have been reconstructed for the LGM, which are globally and

CPD

8, 63–101, 2012

## Sensitivity to glacial boundary conditions

D. Hofer et al.

Title Page

Abstract

Introduction

Conclusions

References

Tables

Figures

◀

▶

◀

▶

Back

Close

Full Screen / Esc

Printer-friendly Version

Interactive Discussion



seasonally resolved (Waelbroeck et al., 2009). Moreover, reconstructions of continental temperature and precipitation are available (e.g., Wu et al., 2007; Allen et al., 2008). Still, in many areas proxy data are sparse and even in some well covered regions as the Nordic Seas discrepancies remain (de Vernal et al., 2006). Consequently, the confidence intervals of reconstructed temperature and precipitation are large.

Nevertheless, the LGM remains the glacial state which is documented the best. The climate in earlier periods of the last glaciation is less understood as proxy data availability is very sparse. Sea level reconstructions indicate changes in the order of several tens of meters during the last glaciation (e.g., Siddall et al., 2008) suggesting strong variations of the total ice mass. For the LGM, the extent and height of the ice sheets are relatively well known (Peltier, 2004), but uncertainties strongly increase when going further back in time. Thus, for the earlier part of the last glacial period the knowledge not only of the climate but also of the lower boundary conditions is limited. One way to overcome these limitations is the use of climate models which allows us to test different settings of the boundary conditions and to investigate their impact on the climate.

Such an approach was already successfully applied to the LGM to evaluate models under strongly altered boundary conditions and to deepen our understanding of the climate system under such extreme conditions. A special effort has been undertaken in the framework of the Paleoclimate Model Intercomparison Project (PMIP) started in the 1990s with atmospheric general circulation models (PMIP1, Joussaume and Taylor, 1995) and continued in its second phase (PMIP2) with atmosphere-ocean general circulation models (Braconnot et al., 2007). The simulations indicate an increasing agreement with the large-scale features of reconstructed temperature fields from PMIP1 to PMIP2. In agreement with reconstructions the largest cooling in the LGM is found over the ice sheets in the Northern Hemisphere (NH) while the tropical ocean shows only weak temperature changes (e.g., Braconnot et al., 2007; Otto-Bliesner et al., 2009). On a more regional scale the results are less consistent, especially in the North Atlantic and the western Europe region, where proxy data (Peyron et al., 1998) indicate lower temperatures than in simulations (Kageyama et al., 2006). The use of higher resolved

## Sensitivity to glacial boundary conditions

D. Hofer et al.

[Title Page](#)[Abstract](#)[Introduction](#)[Conclusions](#)[References](#)[Tables](#)[Figures](#)[◀](#)[▶](#)[◀](#)[▶](#)[Back](#)[Close](#)[Full Screen / Esc](#)[Printer-friendly Version](#)[Interactive Discussion](#)

models can reduce this difference, but does not completely solve the discrepancies (Jost et al., 2005; Ramstein et al., 2007; Kim et al., 2008). A more recent reconstruction, however, suggests that part of the difference is related to the reconstruction methods applied to the proxy data (Wu et al., 2007).

5 Regarding the precipitation, PMIP1 and PMIP2 model results suggest globally drier conditions – due to reduced evaporation as the temperature is lower – except for some mid-latitude areas (Shin et al., 2003; Braconnot et al., 2007). In the NH the precipitation increase especially in winter is related to changes in the storm tracks which overcompensate the general drying (Laine et al., 2009). Previous results for PMIP1 indicated  
10 an eastward shift of the storm tracks in the Atlantic and Pacific with model-dependent characteristics linked to changes in the stationary waves (Kageyama et al., 1999). As common features for four PMIP2 simulations Laine et al. (2009) finds a southeastward shift of the storm track in the North Pacific and a thinning in the western and a south-eastward extension in the eastern part of the North Atlantic. These changes are related  
15 to a similar displacement of the jet stream partly forced by eddies as a consequence of the changed boundary conditions.

In this study, we extend the LGM case studies to an early part of the last glacial period, the Middle Weichselian (MW, 65 ka ago which corresponds to a part of Marine Isotope Stage 4), by utilizing a state-of-the-art atmospheric model forced with prescribed  
20 SSTs and sea ice fields of a lower-resolved but fully coupled model. The MW is chosen because it represents a state which is closer to the beginning of the last glacial period than the LGM, but nevertheless includes a strong glaciation – as suggested by the low sea level compared to other periods in the Early/Middle Weichselian (Siddall et al., 2008). The aim is to examine the influence of different glacial boundary conditions on  
25 the precipitation pattern in the North Atlantic region. This incorporates changes of the ocean surface conditions, the radiative forcing, and the topography. Seven sensitivity time-slice experiments are conducted that differ in at least one of the three parameters. The study focuses on precipitation changes and changes of the atmospheric dynamics.

## Sensitivity to glacial boundary conditions

D. Hofer et al.

Title Page

Abstract

Introduction

Conclusions

References

Tables

Figures

◀

▶

◀

▶

Back

Close

Full Screen / Esc

Printer-friendly Version

Interactive Discussion





## 2.2 Experiments

To investigate the sensitivity of the glacial climate to changes in the boundary conditions a set of time-slice experiments is conducted considering four different periods: present-day (1990 AD), preindustrial (1850 AD), LGM, and MW. An overview of the simulations is presented in Table 1 and the values of the major external forcing factors are summarized in Table 2.

In principle, the simulations are generated as follows: First, a CCSM3 simulation under respective perpetual external forcing conditions is conducted until a sufficiently equilibrated state is reached. The monthly-mean SST and sea ice concentration fields are then interpolated from the irregular ocean grid in CCSM3 to a regular  $0.9^\circ \times 1.25^\circ$  grid and used as time-varying lower boundary conditions for the CCSM4 simulation. Finally, the CCSM4 simulation is conducted for 33 yr and the analysis is based on the last 30 yr of it.

This two-model approach is selected to profit from the results of earlier CCSM3 simulations, which saves computational costs, while still using an up-to-date highly-resolved atmospheric model in the second step. Pre-existing equilibrated CCSM3 simulations are available for all periods except MW; for further information on their settings the reader is referred to Otto-Bliesner et al. (2006a,b) and Brandefelt and Otto-Bliesner (2009). The MW simulation for CCSM3 (hereafter MW3) is initialized from the LGM state in Otto-Bliesner et al. (2006a), which obliges simplifications in the settings of this simulation, namely that the same bathymetry and topography is applied. Thus, the ocean surface includes substantial uncertainties. The MW3 simulation is conducted for 340 yr until equilibrium is reached.

To evaluate the model against reanalysis data (ERA40; Uppala et al., 2005) we apply a different approach, namely a present-day CCSM4 simulation using transient forcings and observational SST and sea ice data for the period 1971 to 2000 (hereafter PDTR; see Hurrell et al. (2008) for information on the SST and sea ice data). The external forcing for PDTR is identical to the one of simulations for the 20th century

### Sensitivity to glacial boundary conditions

D. Hofer et al.

Title Page

Abstract

Introduction

Conclusions

References

Tables

Figures

◀

▶

◀

▶

Back

Close

Full Screen / Esc

Printer-friendly Version

Interactive Discussion



of Gent et al. (2011). The differences between the PDTR and reanalysis data of the same period shed light on the biases of the atmospheric CCSM4 model. Additionally, we perform a time slice simulation for 1990 AD conditions using the two-model approach. Comparing this 1990 AD control simulation (hereafter PD) with the PDTR we quantify the impact of the deviating ocean surface conditions (fully coupled simulated versus observed).

To assess the sensitivity of the glacial climate to changes in the boundary conditions a reference time-slice simulation is needed. In agreement with the PMIP2 protocol a preindustrial simulation with perpetual 1850 AD conditions (hereafter PI) is used as reference.

Then, the sensitivity to the external forcing (orbital and greenhouse gases (GHGs)), to the SST and sea ice distribution and to the ice sheet distribution is investigated in three sets of simulations. The influence of the ocean surface forcing is analysed using two different parts of a LGM simulation that represent a quasi-steady state (LGM13 in Table 1) and the final equilibrium state (LGM23), the latter being 1.1 °C colder in the global mean with much lower SSTs and more extensive sea ice cover in the North Atlantic (Brandefelt and Otto-Bliesner, 2009). To investigate the impact of the radiative forcing (including both changes of the Earth's orbital parameter and of the GHG concentrations) an MW simulation is conducted with the same ice sheet topography as in LGM. Finally, four different ice sheet topographies (Fig. 1, Table 1, and Sect. 2.3) are applied in the MW.

### 2.3 Boundary conditions

For all sensitivity experiments the boundary conditions are set to the same values as in PI except for five parameters: (i) the Earth's orbital parameters, (ii) the concentrations of atmospheric greenhouse gases, (iii) the topography and the coastlines, (iv) the vegetation and the soil type, and (v) the prescribed SST and sea ice fields.

The values for the Earth's orbital parameters are calculated according to Berger (1978). The influence of the different orbital parameters between present-day and

## Sensitivity to glacial boundary conditions

D. Hofer et al.

Title Page

Abstract

Introduction

Conclusions

References

Tables

Figures

◀

▶

◀

▶

Back

Close

Full Screen / Esc

Printer-friendly Version

Interactive Discussion



## Sensitivity to glacial boundary conditions

D. Hofer et al.

Title Page

Abstract

Introduction

Conclusions

References

Tables

Figures

◀

▶

◀

▶

Back

Close

Full Screen / Esc

Printer-friendly Version

Interactive Discussion



preindustrial is neglectable. Compared with today, the solar radiation for the LGM is reduced in both hemispheres during their respective summer with the largest values (up to  $14 \text{ Wm}^{-2}$ ) found in the high-latitudes. For the MW the anomalies are generally larger (up to  $30 \text{ Wm}^{-2}$ ) with lower insolation occurring from March to June (December to April) in the Northern (Southern) Hemisphere and a nearly global positive anomaly centered around September/October. The glacial concentrations of  $\text{CO}_2$ ,  $\text{CH}_4$  and  $\text{N}_2\text{O}$  are based on ice core measurements (Schilt et al. (2010) and B. Bereiter (personal communication, 2011) for MW; PMIP2 protocol for LGM (<http://www-lsce.cea.fr/pmip2/>)). The resulting change of the total radiative forcing relative to preindustrial is  $-2.89 \text{ Wm}^{-2}$  and  $-2.21 \text{ Wm}^{-2}$  for LGM and MW, respectively (estimated according to IPCC (2001, Table 6.2)); the increase from preindustrial to present-day is  $+1.69 \text{ Wm}^{-2}$ .

The topography and the coastlines for all glacial simulations are based on the ICE-5G reconstruction (Peltier, 2004) and they are illustrated in Fig. 1. For the LGM the topography is calculated as the model's present day topography plus the spatially smoothed difference of Peltier's present day and LGM values; the coastline is taken to be at the zero elevation line. For the LGM, the sea-level change corresponds to a decrease of about 120 m with respect to the modern level except for the Caspian Sea which is set to its present-day extent.

For the MW, the ice sheet extent and even more so its thickness are much more uncertain and therefore – and due to a lack of better data – the ICE-5G is used as a starting point for the construction of the ice sheet and the topography. In the five MW simulations the sea-level is lowered by 80 m (Siddall et al., 2008) and the spatial extent of the LGM ice sheet is maintained, while the thickness is adapted individually. Apart from MWLGM, where the original LGM ice sheet height is applied and which is used as sensitivity experiment for the orbital and GHGs forcings, the total ice volume is increased by 2/3 of Peltier's difference (LGM-present day). The spatial distribution is chosen as follows (see also Table 1): (i) in MWLIN all ice sheet heights are increased linearly, (ii) in MWEU the Fennoscandian ice sheet height is increased by 1/3 and the remaining ice sheet by  $\sim 76\%$  of the LGM value, (iii) in MWUS the LGM height is used

except for the Laurentide ice sheet which is at  $\sim 46\%$  of the LGM height, and (iv) in MWNS the same distribution as in MWUS is used and additionally the ice sheet height in the North Sea is set to zero.

The vegetation and the soil type in the glacial simulation are prescribed to the PI distribution except for the additional land areas and the regions that are covered by the grown ice sheet. In the additional land cells vegetation and soil types are set to the mean values of nearby cells and in the ice covered regions the model's standard value for such conditions are used.

### 3 Evaluation

Here, the model's ability to generate a reasonable climate state is investigated. To do so we compare the present-day simulations with reanalysis data and the LGM simulations with reconstructions. This allows identifying biases that have to be considered in the interpretation of the results of the sensitivity experiments.

#### 3.1 Present-day climate state

We focus on the surface air temperature (SAT) and precipitation in the two present-day simulations which are compared to the monthly mean output of the years 1971–2000 of the ERA-40 reanalysis data (Uppala et al., 2005). For the comparison the ERA-40 data is interpolated from a regular  $1^\circ \times 1^\circ$  grid to the  $0.9^\circ \times 1.25^\circ$  resolution of the CCSM4 output.

As expected due to the prescribed observational SSTs, the global mean SAT in PDTR agrees well with ERA-40 data with respect to both the seasonal cycle and the interannual variability (not shown). The simulated global mean temperature is, however,  $0.3^\circ\text{C}$  too low compared to observations. The regional distribution indicates positive biases in the mid-latitudes – especially over Europe and southwestern Russia –, over most of Greenland and some parts of Antarctica, while negative biases are found in the tropics and in high-latitudes with the maximum difference occurring over the sea ice (not shown).

## Sensitivity to glacial boundary conditions

D. Hofer et al.

Title Page

Abstract

Introduction

Conclusions

References

Tables

Figures



Back

Close

Full Screen / Esc

Printer-friendly Version

Interactive Discussion



## Sensitivity to glacial boundary conditions

D. Hofer et al.

Title Page

Abstract

Introduction

Conclusions

References

Tables

Figures

◀

▶

◀

▶

Back

Close

Full Screen / Esc

Printer-friendly Version

Interactive Discussion



In the PD simulation the global mean SAT exhibits an additional bias of  $-0.3^{\circ}\text{C}$  compared to PDTR, which is mainly caused by the too low SST introduced through the fully coupled CCSM3 simulation (see Large and Danabasoglu, 2006, for more information on the SST biases in CCSM3). For SATs over land a similar pattern as in PDTR is found except for a weak warming in the region from  $10^{\circ}\text{S}$  to  $10^{\circ}\text{N}$  (not shown).

The global mean precipitation in PDTR and PD is  $2.92\text{ mm day}^{-1}$  and  $2.90\text{ mm day}^{-1}$ , respectively, which is about 10% less than in ERA-40. However, the precipitation in ERA-40 is known to be excessive especially over the tropical oceans (Uppala et al., 2005, and references therein). This is evident in the difference patterns where the strongest negative biases are located in the tropics (Fig. 2). The tropics are also the area with the most pronounced differences between the two simulations. The diverging precipitation close to the equator in the Pacific and Atlantic are related to biases in the SST forcing of PD due to problems in correctly representing the El Niño-Southern Oscillation in the coupled simulation (Large and Danabasoglu, 2006). Apart from the tropics both simulations exhibit similar patterns with mostly positive anomalies in arid regions and negative anomalies in humid areas.

Overall, SAT and precipitation are simulated reasonably well and the SST biases introduced through CCSM3 do not seem to have a dominant impact on the present day European precipitation.

### 3.2 LGM climate state

Before evaluating the two LGM simulations (LGM1 and LGM2) we investigate our reference simulation (PI) with respect to the PD simulation. The global mean temperature is  $1.25^{\circ}\text{C}$  lower with stronger reductions at high-latitudes. It is not surprising that the global mean SAT difference between PI and PD is much larger than known from observations, as the two simulations represent equilibrated states and the transient climate is not in equilibrium. In contrast to the temperature, the global mean precipitation in PI ( $2.85\text{ mm day}^{-1}$ ) is close to its value in PD. Also the precipitation pattern is not significantly altered except for a weak decrease polewards of  $60^{\circ}$ .

**Sensitivity to glacial boundary conditions**

D. Hofer et al.

Title Page

Abstract

Introduction

Conclusions

References

Tables

Figures

◀

▶

◀

▶

Back

Close

Full Screen / Esc

Printer-friendly Version

Interactive Discussion



The global mean SAT in LGM1 and LGM2 is  $8.02^{\circ}\text{C}$  and  $6.92^{\circ}\text{C}$ , respectively (compared to  $12.47^{\circ}\text{C}$  for PI). Due to the sparse proxy data for LGM the global mean cannot be directly compared to reconstruction. The amplitude of the cooling is consistent with other models, e.g., a model comparison of six fully-coupled PMIP2 simulations shows a range of  $-3.6$  to  $-5.7^{\circ}\text{C}$  (Braconnot et al., 2007, note that one of the models is CCSM3 so that the results are not fully independent). The simulated cooling is more pronounced in the mid- and high-latitudes with a maximum in the order of  $-30^{\circ}\text{C}$  over the Laurentide and Fennoscandian ice sheets (Fig. 3a and c). Temperatures in the tropical regions are less affected and the changes are generally smaller than  $5^{\circ}\text{C}$ . Overall, the large-scale SAT patterns in our LGM simulations are consistent with the multi-model mean of Braconnot et al. (2007) apart from anomalies in the North Pacific (too warm in LGM1) and the North Atlantic (too cold in LGM2 and partly also in LGM1) which are related to biases in the ocean surface forcing.

As shown by Otto-Bliesner et al. (2006a) for the not equilibrated CCSM3 LGM state, the SSTs are too high in the North Pacific north of  $50^{\circ}\text{N}$  and too low in the high-latitude North Atlantic compared to proxy data. In winter (December-January-February, DJF) they showed that the extent of sea ice is overestimated in the western Atlantic at  $45^{\circ}\text{N}$  (Fig. 3c). For the equilibrated LGM state Brandefelt and Otto-Bliesner (2009) find even lower SSTs in the North Atlantic and the Nordic Seas and much more extended sea ice in the North Atlantic region both in summer (June-July-August, JJA) and winter (Fig. 3a and b). In addition to these large-scale biases induced by CCSM3, temperatures at oceanic edges around major ice sheets are increased relative to its surrounding. This has not been reported for other LGM simulations. The reasons are persistent and strong catabatic winds which lead to an increase of the SAT at the boundary of the ice sheets. As the effect is spatially limited and much smaller than the SST biases it is not considered any further.

The global mean precipitation is reduced from  $2.85\text{ mm day}^{-1}$  in PI to  $2.56\text{ mm day}^{-1}$  and  $2.50\text{ mm day}^{-1}$  in LGM1 and LGM2, respectively. Regionally, precipitation anomalies between  $30^{\circ}\text{S}$  and  $30^{\circ}\text{N}$  are pronounced (up to  $5\text{ mm day}^{-1}$ ) in both LGM simu-

lations, but not uniform in sign. However, the mid- and high-latitudes generally exhibit drier conditions (Fig. 3b and d). Outside of the tropics positive anomalies occur only in the NH, namely at the western coast of Europe and North America, in a band at 35° N across most of the Atlantic and in some regions at the edges of the major ice sheets. As for SAT the large-scale precipitation anomaly patterns are consistent with the multi-model mean of Braconnot et al. (2007).

The simulated LGM climate in Europe is also compared to the reconstruction from Wu et al. (2007) which is based on an inverse vegetation modelling approach using pollen data. The reconstruction offers temperature and precipitation anomalies with respect to the 1970s for the coldest (January) and warmest (July) month and for the annual mean. 32 sites in the European region are selected and compared with the simulated pattern of LGM1/LGM2-PD.

For the coldest month the SAT patterns exhibit a strong meridional gradient which is found in reconstructed data over Eurasia (Wu et al., 2007), but not clearly evident over Europe (Fig. 4a and b). Thus, the cooling is underestimated for most of the southern locations, while it is overestimated for the northern part. Nevertheless, the temperature difference between the simulations and the reconstruction is less than 5 °C for the majority of the proxy sites and it is only significant at few locations.

The simulated SAT patterns for the warmest month are less zonal with decreasing temperature differences from the northwest to the southeast (Fig. 4c and d). At most locations the simulated SATs are outside the 90 % confidence interval of the reconstruction with a tendency towards overestimated temperature differences. Thus, the simulations' results for summer should be interpreted with caution.

For the annual mean SAT the simulations are close to the reconstruction in the Mediterranean region as the overestimated cooling in summer is compensated by the underestimated cooling in winter (Fig. 4e and f). The offset in the far northeast is, however, still in the order of 10 °C.

In all three cases strong temperature differences at nearby proxy sites, which are likely related to locale impact factors, have no correspondence in the simulated pattern.

## Sensitivity to glacial boundary conditions

D. Hofer et al.

Title Page

Abstract

Introduction

Conclusions

References

Tables

Figures

◀

▶

◀

▶

Back

Close

Full Screen / Esc

Printer-friendly Version

Interactive Discussion



## Sensitivity to glacial boundary conditions

D. Hofer et al.

Title Page

Abstract

Introduction

Conclusions

References

Tables

Figures

◀

▶

◀

▶

Back

Close

Full Screen / Esc

Printer-friendly Version

Interactive Discussion



For the precipitation the uncertainties in the reconstruction are large so that only at one location in the Pyrenees the anomaly is significantly different from the present (Wu et al., 2007). The reconstruction indicates a tendency towards drier conditions over Europe for the annual mean, as well as the coldest and warmest month, while the simulations exhibit a more heterogeneous pattern with a band between 35° to 50° N of increased precipitation in January and one between 50° to 60° N in July (Fig. 5). Due to the large uncertainties the simulated precipitation anomalies are though consistent with the reconstruction at most locations. Note, however, that the strongly increased winter precipitation in Spain has no analogue in the reconstruction.

To summarize the large-scale feature of the simulated SAT and precipitation anomaly patterns for LGM are consistent with the multi-model mean of six fully coupled AOGCMs. In the European region the results are mostly within the large confidence intervals of reconstructed continental temperature and precipitation anomalies except for summer SATs. No evidence is found that one of the two LGM simulations leads to a much better agreement with the reconstruction, as the SATs agree better in LGM1 while precipitation agrees more in LGM2.

## 4 Impact on temperature and precipitation

### 4.1 Sensitivity to the ocean surface and the radiative forcing

The climate state in the three simulations that have the LGM ice sheet height implemented (LGM1, LGM2 and MWLGM) are compared for the North Atlantic region to investigate the influence of differences either in the ocean surface forcing or in the radiative forcing. The first is evaluated by comparing the two LGM simulations which differ only in their prescribed time-varying SSTs and sea ice forcing while the latter is estimated as the difference between the equilibrium states for LGM and MW. As noted in the experimental description the differences in the radiative forcing consists of changes in the GHG concentrations and in the orbital parameters of the Earth.

## Sensitivity to glacial boundary conditions

D. Hofer et al.

Title Page

Abstract

Introduction

Conclusions

References

Tables

Figures

◀

▶

◀

▶

Back

Close

Full Screen / Esc

Printer-friendly Version

Interactive Discussion



The annual mean SAT difference patterns between LGM1/LGM2 and PI agree on the major characteristics of the changes (Fig. 3a and c and Sect. 3.2). As expected from the prescribed ocean surface forcing, the strongest discrepancies between the simulations occur in the North Atlantic region for DJF. In LGM2 the winter sea ice extends as far south as 40° N and the Nordic Seas are widely covered by ice leading to a strong regional decrease of SATs compared to PI (Fig. 6a). In contrast, the less extensive southward sea ice extent in LGM1 leads to a much less pronounced cooling, so that the two LGM simulations differ by up to 30°C over the ocean especially in the Nordic Seas (Fig. 6b). As a further consequence the cooling in Europe which lies downstream of the strong anomaly is less pronounced in LGM1. For JJA the temperature anomalies are weaker and the differences between the two LGM simulations are generally less than 5°C, but they are still statistically significant at the 5% level (Fig. 6d and e).

As for the temperature the large-scale annual mean precipitation anomaly patterns of the LGM simulations with respect to PI agree well (Fig. 3b and d). In the North Atlantic region the anomaly patterns for DJF and JJA share the main characteristics, namely generally drier conditions except for a band of increased precipitation between 30° to 40° N reaching from the eastern coast of North America to the Mediterranean in winter and for some tropical region and parts of the Fennoscandian ice sheet in summer (Fig. 7a–d). Note that positive winter precipitation anomalies in southwestern Europe and the adjacent Atlantic are a common feature of LGM simulations of different models (Laine et al., 2009) and are also found in CCSM3 (Strandberg et al., 2011). At most locations in the mid- and high-latitudes the anomalies are larger in winter than in summer and the differences between LGM1 and LGM2 are more pronounced in winter (Fig. 7g and h). Compared to LGM2 the DJF precipitation in LGM1 is increased in the northern North Atlantic, in the Nordic Seas, and in parts of the Mediterranean, while a decrease is found at the lee side of the Fennoscandian ice sheet. In summer, most of the differences are not significant (at the 5% level) except for the area from the eastern coast of Greenland to central and eastern Europe where in LGM1 slightly wetter conditions prevail.

## Sensitivity to glacial boundary conditions

D. Hofer et al.

Title Page

Abstract

Introduction

Conclusions

References

Tables

Figures

◀

▶

◀

▶

Back

Close

Full Screen / Esc

Printer-friendly Version

Interactive Discussion



The impact of the radiative forcing changes between the LGM and MW show a more complex picture. The global mean SAT in MWLGM is 7.71 °C which is 0.8 °C higher than in LGM2, but slightly lower than in LGM1, and the annual mean SAT pattern is close to the ones in the LGM simulations (Fig. 3e). As the northeastern part of the Atlantic and the Nordic Seas are only partially covered by sea ice in winter, the strongest anomalies with respect to LGM2 are located in this region (Fig. 6c). Generally, the anomaly pattern is similar to the one for LGM1, but with reduced amplitude especially around Newfoundland. Due to the strong ocean surface differences north of 40° N, which represent the forcing impacts in CCSM3, it is impossible to estimate the direct effect of the orbital and GHGs changes on the CCSM4 atmosphere in this region. Elsewhere the changes correspond to the forcing, i.e. the SH is slightly cooler in MWLGM due to a strong reduction of solar insolation that overcompensates the increased GHGs forcing. For JJA, the SATs are globally higher in MWLGM in agreement with the higher insolation and the increased GHG concentrations (Fig. 6f).

The global mean precipitation in MWLGM is of similar strength as in LGM1 (2.56 mm day<sup>-1</sup>). The spatial distributions of the anomalies with respect to PI resembles the ones of the LGM simulations for the annual mean (Fig. 3f) as well as for DJF and JJA (Fig. 7e and f). The winter precipitation difference pattern LGM2-MWLGM is similar to the pattern LGM2-LGM1, but with reduced amplitudes especially in the surrounding of Newfoundland (Fig. 3i). In contrast, for summer precipitation the pattern of LGM2-MWLGM differs from the one of LGM2-LGM1 showing a strong negative difference in the tropical Atlantic region and a northward shift of the significant mid- and high-latitude changes (Fig. 3j).

Overall, the different ocean surface forcings for LGM1 and LGM2 do not fundamentally alter the large-scale precipitation anomaly patterns compared to PI, even though the impact on winter SATs is strong. The main difference between the simulations is a modulation of the amplitude in several regions, e.g. in the Nordic Seas. The effect of the changed radiative forcing in MWLGM globally affects SATs and also the precipitation in the tropics, but it is not possible to directly address its impact on the precipitation

in the North Atlantic region as the major differences seen in this region can be at least partly related to changes in the ocean surface.

## 4.2 Sensitivity to ice sheet height

The impact of the topography on the atmospheric dynamic and the precipitation pattern is investigated using the four MW sensitivity simulations (MWLIN, MWEU, MWUS and MWNS). Note that the total ice sheet volume change in these sensitivity experiments corresponds to the sea level change of 80 m. The differences found will be compared to the results obtained in the last section.

Due to the topography changes which result in a reduced mean altitude, the global mean SATs in the four simulations are slightly higher than in MWLGM ranging from 7.73 °C to 7.78 °C. As in the other three glacial simulations, the strongest changes of the annual mean SATs compared to PI are found over the NH ice sheets while the anomalies in the tropics are weak (not shown). In contrast to the LGM cases, significant SAT differences between the simulations occur over the ice sheets as a direct effect of the changed altitude and – especially in winter – in continental regions downstream of the ice sheets (not shown). The only significant difference between the MW simulations over the ocean is a warming (compared to MWLGM) in winter between 40° and 50° N across the North Atlantic that is most pronounced in MWUS and MWNS reaching up to 8 °C (not shown).

The global mean precipitation is not affected by the topography changes and does not differ by more than 0.01 mm day<sup>-1</sup> in the MW simulations. Regarding winter precipitation, however, a strong impact of the height of the ice sheets is evident (Fig. 8). The band of positive precipitation anomalies in the mid-latitudes, that occurs in all three simulations with the LGM topography applied, is reduced and the reduction is stronger the more the Laurentide ice sheet is lowered. While the significant anomalies are only slightly diluted in MWEU (Laurentide ice sheet height at 76 % of the LGM value), they are strongly reduced in MWLIN (height at 67 %) especially in the eastern part and do no longer form a continuous band. In MWUS and MWNS (height at 46 %) the positive

## Sensitivity to glacial boundary conditions

D. Hofer et al.

Title Page

Abstract

Introduction

Conclusions

References

Tables

Figures

◀

▶

◀

▶

Back

Close

Full Screen / Esc

Printer-friendly Version

Interactive Discussion



## Sensitivity to glacial boundary conditions

D. Hofer et al.

Title Page

Abstract

Introduction

Conclusions

References

Tables

Figures

◀

▶

◀

▶

Back

Close

Full Screen / Esc

Printer-friendly Version

Interactive Discussion



precipitation anomalies are limited to the western part between 40° W to 70° W except for a few small patches around Spain in MWUS. The discrepancy between MWUS and MWNS around Spain is attributed to internal variability, as the difference between the two simulations is not significant in this region (not shown). Additionally, precipitation anomalies in other areas consistently change with the height of the Laurentide ice sheet. A lower altitude of the Laurentide ice sheet corresponds to a precipitation increase over the eastern part of its slope, in the Labrador Sea and in the North Atlantic at 20° N. The impact of the Fennoscandian ice sheet is less pronounced and mainly affects the precipitation at its southeastern slope. There, the precipitation is significantly increased in the simulations with a lowered altitude of the Fennoscandian ice sheet compared to MWLGM while no significant changes are found for MWUS and MWNS (not shown).

For summer precipitation the differences between the four simulations are much smaller and not significant for most regions (Fig. 8). The few significant changes point to a similar but much weaker impact of the Laurentide ice sheet as in winter with increased precipitation in the high-latitudes and a band of reduced precipitation across the Atlantic compared to MWLGM, but overall the anomaly patterns are similar for all MW simulations.

Analysing the MW simulations indicates a strong impact of the topography on the winter precipitation pattern. For most of the anomalies in the North Atlantic region the height of the Laurentide ice sheet is identified as the dominant factor. Together with the changed winter SATs over the North Atlantic – even though the lower boundary forcing is the same – the results suggest a change of the atmospheric dynamics.

### 5 Importance of the atmospheric dynamics

Other studies have shown that the DJF precipitation anomalies in LGM simulations are related to changes in the storminess (Laine et al., 2009) and for CCSM3 the increased mid-latitude LGM precipitation is associated with a southward shift of the Atlantic storm track (Otto-Bliesner et al., 2006a; Strandberg et al., 2011). To investigate the impact of

the boundary conditions on the synoptic scale variability in our simulations two different methods are considered: an Eulerian measure, which is defined as the bandpass filtered (2.5–6 days) standard deviation of the 500 hPa geopotential height (Blackmon, 1976) and a Lagrangian method, where the storminess is estimated based on the trajectories of low-pressure systems at 1000 hPa geopotential height (Blender et al., 1997). Both methods are applied to 6-hourly data. For the Lagrangian approach only low-pressure systems are considered that have a life-time of at least one day and whose mean gradients around the minimum (radius of 1000 km) exceed 100 gpm per 1000 km during the life cycle. Additionally, cyclones in regions where the terrain height is above 1000 m are excluded due to potential extrapolation errors in the 1000 hPa geopotential height field.

For PI the storm track and the cyclone track density patterns are similar to the ones found for present-day observations (Fig. 9a; e.g., Raible et al., 2008). The Eulerian measure exhibits a maximum over Newfoundland extending eastwards to the ocean and the cyclone track density is high in the region from the northwestern North Atlantic to the south of Greenland, around Iceland and in the Nordic Seas. In the glacial simulations the anomalies for both measures indicate a southward shift with a decrease in the north and northwestern part and an increase in the south (Fig. 9b–h). For the Eulerian measure the anomalies form a dipole like structure with the minimum located around the southern tip of Greenland and the maximum lying west of Spain while the cyclone track density indicate a similar pattern, but shifted to the north. Generally, the anomalies are strongest when using the full LGM ice sheet height and decrease with a lower Laurentide ice sheet.

Some differences between the LGM1, LGM2 and MWLGM simulations are notable suggesting an influence of the ocean surface forcing. In LGM2 – and to a lesser degree in MWLGM – the amplitudes of the anomalies over the North Atlantic are increased compared to LGM1. Such a behavior is expected as a consequence of the stronger SAT reduction in the northern part which increases the meridional temperature gradient at the surface leading to enhanced lower-level baroclinicity.

## Sensitivity to glacial boundary conditions

D. Hofer et al.

[Title Page](#)[Abstract](#)[Introduction](#)[Conclusions](#)[References](#)[Tables](#)[Figures](#)[◀](#)[▶](#)[◀](#)[▶](#)[Back](#)[Close](#)[Full Screen / Esc](#)[Printer-friendly Version](#)[Interactive Discussion](#)

**Sensitivity to glacial boundary conditions**

D. Hofer et al.

Title Page

Abstract

Introduction

Conclusions

References

Tables

Figures

◀

▶

◀

▶

Back

Close

Full Screen / Esc

Printer-friendly Version

Interactive Discussion



In the case of a lower Laurentide ice sheet the anomalies are not only weaker, but also changed in their structure (Fig. 9e–h). The dipole like pattern of the bandpass filtered standard deviation of the 500 hPa geopotential height is reduced in MWLIN and MWEU and nearly vanishes in MWUS and MWNS. For the latter the remaining anomalies over the Atlantic are located more to the north. Similarly, the positive anomalies of the cyclone track density are shifted to the north and reduced to patches in the western Atlantic at 35° N and the region around the Iceland-Scotland ridge (again more so in MWNS and MWUS than in MWLIN and MWEU). In contrast, a clear impact of the Fennoscandian ice sheet is only evident in the very eastern (30–60° E) mid-latitudes where the anomalies mostly vanish for MWEU.

To complete the analysis of the atmospheric dynamics the changes in the upper troposphere are investigated. To do so the zonal wind at 200 hPa – the height of the jet stream maximum – is examined. In PI the jet develops two branches in the North Atlantic the so-called eddy driven jet which extends from the eastern coast of North America to Great Britain and the subtropical jet which is located at 20° to 30° N across the entire sector with the maximum wind speed in its eastern part (Fig. 10a). In the glacial simulations this pattern strongly changes with increasing height of the Laurentide ice sheet: The southern part of the jet is weakened while the wind speed in the central North Atlantic is strongly increased (Fig. 10b–h). This corresponds to a strengthening and southward extension of the eddy-driven jet and – especially in LGM1, LGM2 and MWLGM – to a interruption of the subtropical jet over the Atlantic (not shown). As for the storm and cyclone tracks the changes are amplified by the increased meridional temperature gradient in LGM2. In simulations with a lower Laurentide ice sheet the anomalies are not only weaker, but also shifted to the north. Over the Fennoscandian ice sheet we see an enhanced zonal wind in MWUS and MWNS, which is most pronounced in spring and autumn (not shown). Given the available simulations it is, however, not possible to determine whether this is a feature of the interplay between the two ice sheets or only related to the Fennoscandian one.

The atmospheric dynamics in summer is also changed but not as strong as in winter. Both measures for the storminess indicate a tendency towards increased synoptic activity in the south and a decrease in the northwest which are stronger in the simulations with a high Laurentide ice sheet (not shown). However, the jet stream is not displaced in summer (not shown).

## 6 Discussion and conclusions

Using the ocean surface conditions of simulations with a fully coupled AOGCM (CCSM3) as input to a higher resolved atmospheric general circulation model (CCSM4) we investigated the impact of different glacial boundary conditions on the temperature, precipitation, and atmospheric dynamics in the North Atlantic region. The two-model approach is selected as it is a very computational effective way to investigate the problem, especially because equilibrium simulations for the present-day, the preindustrial period, and the LGM conducted with CCSM3 were already available (Otto-Bliesner et al., 2006a; Brandefelt and Otto-Bliesner, 2009).

However, the approach imposes new uncertainties as biases and shortcomings in the low-resolution simulations are introduced in the high-resolution CCSM4 and the ocean response to the applied atmospheric forcing within CCSM4 is neglected. Fortunately, the analysis has shown that even the strong differences between the ocean surface forcing in LGM1 and LGM2 do not fundamentally alter the resulting large-scale patterns but mainly affect the regional climate. We therefore conclude that the approach used in this study is reasonable even though the ocean surface in the CCSM4 simulations has potential deficiencies.

Before the differences between the glacial simulations are investigated, the model's ability to simulate present-day and LGM climates is evaluated. Even though in many regions temperature and precipitation in the model significantly differ from the reanalysis data for present-day (which is, however, partially attributed to problems in the reanalysis data, Uppala et al., 2005), these biases are much weaker than the anomalies between the recent past and the glacial states for the North Atlantic region. Therefore,

## Sensitivity to glacial boundary conditions

D. Hofer et al.

Title Page

Abstract

Introduction

Conclusions

References

Tables

Figures



Back

Close

Full Screen / Esc

Printer-friendly Version

Interactive Discussion



we are confident that the glacial differences are not caused by biases that are already present in the present-day simulations. The glacial anomalies for summer should, however, be interpreted with caution as the amplitudes are generally smaller and – more importantly – the simulated July SATs for LGM are outside the confidence intervals of the reconstruction of Wu et al. (2007) at most locations. For winter the LGM simulations mostly lies within the confidence intervals of the reconstruction with one exception over southwestern Europe. There, the simulations indicate strong positive winter precipitation anomalies while the reconstruction show a slight decrease. These differences are possibly related to locale factors because the proxies sites are located in mountainous regions that are not fully resolved in the model. Note, however, that the proxy data has a large confidence interval and that other models – including a regional one with higher resolution – find also a precipitation increase over this region (Braconnot et al., 2007; Strandberg et al., 2011).

Even though the LGM simulations widely agree with the reconstruction it is important to note that they have substantial uncertainties included: The extent and altitude of the ice sheets are only approximations and several forcing factors are missing, e.g., changes of the vegetation cover and dust. Other studies have shown that for the LGM changed vegetation and dust can alter global SATs in the order of several tenth of a degree C each (Jahn et al., 2005; Mahowald et al., 2006). An additional source of uncertainties is introduced through the prescribed ocean surface conditions which have several biases compared to reconstructions (Otto-Bliesner et al., 2006a; Brandefelt and Otto-Bliesner, 2009). The ocean surface biases are expected to be worse in the MW simulations, as the CCSM3 simulation for MW uses the LGM bathymetry and topography that do not represent the MW conditions correctly. However, the preferential intent of this study is not to simulate the climate for MW with the highest accuracy possible, but to investigate the sensitivity of the climate to different glacial boundary conditions. Thus, all of the MW simulations have to be understood as sensitivity experiments based on the MW state more than as accurate representations of the MW climate.

## Sensitivity to glacial boundary conditions

D. Hofer et al.

[Title Page](#)[Abstract](#)[Introduction](#)[Conclusions](#)[References](#)[Tables](#)[Figures](#)[◀](#)[▶](#)[◀](#)[▶](#)[Back](#)[Close](#)[Full Screen / Esc](#)[Printer-friendly Version](#)[Interactive Discussion](#)

**Sensitivity to glacial boundary conditions**

D. Hofer et al.

Title Page

Abstract

Introduction

Conclusions

References

Tables

Figures

◀

▶

◀

▶

Back

Close

Full Screen / Esc

Printer-friendly Version

Interactive Discussion



Our glacial experiments have shown that especially in winter the climate in the North Atlantic region is strongly influenced by the altitude of the Laurentide ice sheet. A high ice sheet (as in LGM) leads to a southward shift of the eddy-driven jet stream and of the storm and cyclone track, which is more pronounced in the eastern part of the North Atlantic. This resembles findings of other PMIP1 and PMIP2 simulations that exhibit a southeastward extension of the winter storm track (Kageyama et al., 1999; Laine et al., 2009). In our simulations we find a direct relationship between changes in the storm track and precipitation anomalies in the North Atlantic region. However, our study is based on only one model and the results of Laine et al. (2009) suggest that such a relationship could be model-dependent.

The analysis of the two LGM simulations with different ocean surface forcings shows that the observed atmospheric changes for a high Laurentide ice sheet are amplified when the meridional temperature gradient in the North Atlantic is increased. This result is consistent with Toracinta et al. (2004) who used a lower resolved atmospheric model forced either by the CLIMAP SST fields or by artificially adapted CLIMAP SST fields with a lower meridional temperature gradient. An analogue behavior, namely a southward shift of the storm track in the North Atlantic, is also reported for a modeling study comparing the Little Ice Age (1550–1850 AD) with present-day which shows an increased meridional temperature gradient (Raible et al., 2007).

The impact of the radiative forcing difference between LGM and MW in the time slice experiments is dominated by the lower boundary conditions introduced by the fully-coupled CCSM3. Thus, the impacts on atmospheric dynamics and precipitation as well as the mechanism are similar to the ones for the ocean surface forcing.

*Acknowledgements.* We gratefully acknowledge Niklaus Merz for valuable discussion. This work is funded by the Swiss Federal Nuclear Safety Inspectorate (ENSI). CCR is supported by the NCCR Climate and the EU project Past4Future. Most simulations were performed at the Swiss National Supercomputing Centre (CSCS) in Manno. Some simulations and model data were kindly made available by the NCAR and by Jenny Brandefelt.

## References

- Allen, R., Siegert, M. J., and Payne, A. J.: Reconstructing glacier-based climates of LGM Europe and Russia Part 2: A dataset of LGM precipitation/temperature relations derived from degree-day modelling of palaeo glaciers, *Clim. Past*, 4, 249–263, doi:10.5194/cp-4-249-2008, 2008. 65
- Berger, A. L.: Long-term variations of daily insolation and quaternary climatic changes, *J. Atmos. Sci.*, 35, 2362–2367, 1978. 69, 91
- Blackmon, M. L.: Climatological Spectral Study of 500 Mb Geopotential Height of Northern Hemisphere, *J. Atmos. Sci.*, 33, 1607–1623, 1976. 80
- Blender, R., Fraedrich, K., and Lunkeit, F.: Identification of cyclone-track regimes in the North Atlantic, *Q. J. Roy. Meteorol. Soc.*, 123, 727–741, doi:10.1002/qj.49712353910, 1997. 80
- Braconnot, P., Otto-Bliesner, B., Harrison, S., Joussaume, S., Peterchmitt, J.-Y., Abe-Ouchi, A., Crucifix, M., Driesschaert, E., Fichet, Th., Hewitt, C. D., Kageyama, M., Kitoh, A., Laîné, A., Loutre, M.-F., Marti, O., Merkel, U., Ramstein, G., Valdes, P., Weber, S. L., Yu, Y., and Zhao, Y.: Results of PMIP2 coupled simulations of the Mid-Holocene and Last Glacial Maximum – Part 1: experiments and large-scale features, *Clim. Past*, 3, 261–277, doi:10.5194/cp-3-261-2007, 2007. 65, 66, 73, 74, 83
- Brandefelt, J. and Otto-Bliesner, B. L.: Equilibration and variability in a Last Glacial Maximum climate simulation with CCSM3, *Geophys. Res. Lett.*, 36, L19712, doi:10.1029/2009GL040364, 2009. 68, 69, 73, 82, 83, 90
- Collins, W. D., Bitz, C. M., Blackmon, M. L., Bonan, G. B., Bretherton, C. S., Carton, J. A., Chang, P., Doney, S. C., Hack, J. J., Henderson, T. B., Kiehl, J. T., Large, W. G., McKenna, D. S., Santer, B. D., and Smith, R. D.: The Community Climate System Model version 3 (CCSM3), *J. Climate*, 19, 2122–2143, 2006. 67
- de Vernal, A., Rosell-Mele, A., Kucera, M., Hillaire-Marcel, C., Eynaud, F., Weinelt, M., Dokken, T., and Kageyama, M.: Comparing proxies for the reconstruction of LGM sea-surface conditions in the northern North Atlantic, *Quater. Sci. Rev.*, 25, 2820–2834, doi:10.1016/j.quascirev.2006.06.006, 2006. 65
- Gent, P. R., Danabasoglu, G., Donner, L. J., Holland, M. M., Hunke, E. C., Jayne, S. R., Lawrence, D. M., Neale, R. B., Rasch, P. J., Vertenstein, M., Worley, P. H., Yang, Z. L., and M., Z.: The Community Climate System Model version 4, *J. Climate*, 24, 19, 4973–4991, doi:10.1175/2011JCLI4083.1, 2011. 69

## Sensitivity to glacial boundary conditions

D. Hofer et al.

Title Page

Abstract

Introduction

Conclusions

References

Tables

Figures

◀

▶

◀

▶

Back

Close

Full Screen / Esc

Printer-friendly Version

Interactive Discussion



**Sensitivity to glacial boundary conditions**

D. Hofer et al.

Title Page

Abstract

Introduction

Conclusions

References

Tables

Figures

◀

▶

◀

▶

Back

Close

Full Screen / Esc

Printer-friendly Version

Interactive Discussion



- Hunke, E. C. and Lipscomb, W. H.: CICE: The Los Alamos sea ice model users manual, version 4, Los Alamos National Laboratory Tech. Rep. LA-CC-06-012, 76 pp., 2008. 67
- Hurrell, J. W., Hack, J. J., Shea, D., Caron, J. M., and Rosinski, J.: A new sea surface temperature and sea ice boundary dataset for the Community Atmosphere Model, *J. Climate*, 21, 5145–5153, doi:10.1175/2008JCLI2292.1, 2008. 68
- IPCC: Climate Change 2001: The Scientific Basis. Contribution of Working Group I to the Third Assessment Report of the Intergovernmental Panel on Climate Change, Cambridge University Press, Cambridge, United Kingdom and New York, NY, USA, 2001. 70
- Jahn, A., Claussen, M., Ganopolski, A., and Brovkin, V.: Quantifying the effect of vegetation dynamics on the climate of the Last Glacial Maximum, *Clim. Past*, 1, 1–7, doi:10.5194/cp-1-1-2005, 2005. 83
- Jost, A., Lunt, D., Kageyama, M., Abe-Ouchi, A., Peyron, O., Valdes, P. J., and Ramstein, G.: High-resolution simulations of the last glacial maximum climate over Europe: a solution to discrepancies with continental palaeoclimatic reconstructions?, *Clim. Dynam.*, 24, 577–590, doi:10.1007/s00382-005-0009-4, 2005. 66
- Joussaume, S. and Taylor, K. E.: Status of the paleoclimate modeling intercomparison project (PMIP), in: Proceedings of the first international AMIP scientific conference, 425–430, WCRP-92, Monterey, USA, 1995. 65
- Kageyama, M., Valdes, P. J., Ramstein, G., Hewitt, C., and Wyputta, U.: Northern hemisphere storm tracks in present day and last glacial maximum climate simulations: A comparison of the European PMIP models, *J. Climate*, 12, 742–760, 1999. 66, 84
- Kageyama, M., Laine, A., Abe-Ouchi, A., Braconnot, P., Cortijo, E., Crucifix, M., de Vernal, A., Guiot, J., Hewitt, C. D., Kitoh, A., Kucera, M., Marti, O., Ohgaito, R., Otto-Bliesner, B., Peltier, W. R., Rosell-Mele, A., Vettoretti, G., Weber, S. L., and Yu, Y.: Last Glacial Maximum temperatures over the North Atlantic, Europe and western Siberia: a comparison between PMIP models, MARGO sea-surface temperatures and pollen-based reconstructions, *Quatern. Sci. Rev.*, 25, 2082–2102, doi:10.1016/j.quascirev.2006.02.010, 2006. 65
- Kim, S. J., Crowley, T. J., Erickson, D. J., Govindasamy, B., Duffy, P. B., and Lee, B. Y.: High-resolution climate simulation of the last glacial maximum, *Clim. Dynam.*, 31, 1–16, doi:10.1007/s00382-007-0332-z, 2008. 66
- Laine, A., Kageyama, M., Salas-Melia, D., Voldoire, A., Riviere, G., Ramstein, G., Planton, S., Tyteca, S., and Peterschmitt, J. Y.: Northern hemisphere storm tracks during the last glacial maximum in the PMIP2 ocean-atmosphere coupled models: energetic study, seasonal cycle,

**Sensitivity to glacial boundary conditions**

D. Hofer et al.

Title Page

Abstract

Introduction

Conclusions

References

Tables

Figures

◀

▶

◀

▶

Back

Close

Full Screen / Esc

Printer-friendly Version

Interactive Discussion



precipitation, *Clim. Dynam.*, 32, 593–614, doi:10.1007/s00382-008-0391-9, 2009. 66, 76, 79, 84

Large, W. G. and Danabasoglu, G.: Attribution and impacts of upper-ocean biases in CCSM3, *J. Climate*, 19, 2325–2346, 2006. 72

5 Mahowald, N. M., Yoshioka, M., Collins, W. D., Conley, A. J., Fillmore, D. W., and Coleman, D. B.: Climate response and radiative forcing from mineral aerosols during the last glacial maximum, pre-industrial, current and doubled-carbon dioxide climates, *Geophys. Res. Lett.*, 33, L20705, doi:10.1029/2006GL026126, 2006. 83

10 Neale, R. B., Richter, J. H., Conley, A. J., Park, S., Lauritzen, P. H., Gettelman, A., a. W. D. L., Rasch, P. J., Vavrus, S. J., Taylor, M. A., Collins, W. D., Zhang, M., and Lin, S.: Description of the NCAR Community Atmosphere Model (CAM4), National Center for Atmospheric Research Tech. Rep. NCAR/TN+STR, 194 pp., 2010. 67

15 Oleson, K., Lawrence, D., Bonan, G., Flanner, M., Kluzek, E., Lawrence, P., Levis, S., Swenson, S., Thornton, P., Dai, A., Decker, M., Dickinson, R., Feddema, J., Heald, C., F. Hoffman, a. J.-F. L., Mahowald, N., Niu, G.-Y., Qian, T., Randerson, J., Running, S., Sakaguchi, K., Slater, A., Stockli, R., Wang, A., Yang, Z.-L., Zeng, X., and Zeng, X.: Technical Description of version 4.0 of the Community Land Model (CLM), NCAR Technical Note NCAR/TN-478+STR, National Center for Atmospheric Research, Boulder, CO, 257 pp., 2010. 67

20 Otto-Bliesner, B. L., Brady, E. C., Clauzet, G., Tomas, R., Levis, S., and Kothavala, Z.: Last Glacial Maximum and Holocene climate in CCSM3, *J. Climate*, 19, 2526–2544, doi:10.1175/JCLI3748.1, 2006a. 67, 68, 73, 79, 82, 83, 90

Otto-Bliesner, B. L., Tomas, R., Brady, E. C., Ammann, C., Kothavala, Z., and Clauzet, G.: Climate sensitivity of moderate- and low-resolution versions of CCSM3 to preindustrial forcings, *J. Climate*, 19, 2567–2583, doi:10.1175/JCLI3754.1, 2006b. 68, 90

25 Otto-Bliesner, B. L., Schneider, R., Brady, E. C., Kucera, M., Abe-Ouchi, A., Bard, E., Braconnot, P., Crucifix, M., Hewitt, C. D., Kageyama, M., Marti, O., Paul, A., Rosell-Mele, A., Waelbroeck, C., Weber, S. L., Weinelt, M., and Yu, Y.: A comparison of PMIP2 model simulations and the MARGO proxy reconstruction for tropical sea surface temperatures at last glacial maximum, *Clim. Dynam.*, 32, 799–815, doi:10.1007/s00382-008-0509-0, 2009. 65

30 Peltier, W. R.: Global glacial isostasy and the surface of the ice-age earth: The ice-5G (VM2) model and grace, *Annu. Rev. Earth Pl. Sc.*, 32, 111–149, 2004. 65, 70, 92

Peyron, O., Guiot, J., Cheddadi, R., Tarasov, P., Reille, M., de Beaulieu, J. L., Bottema, S., and Andrieu, V.: Climatic reconstruction in Europe for 18 000 yr B.P. from pollen data, *Quatern.*

## Sensitivity to glacial boundary conditions

D. Hofer et al.

Title Page

Abstract

Introduction

Conclusions

References

Tables

Figures

◀

▶

◀

▶

Back

Close

Full Screen / Esc

Printer-friendly Version

Interactive Discussion



Res., 49, 183–196, 1998. 65

Raible, C. C., Yoshimori, M., Stocker, T. F., and Casty, C.: Extreme midlatitude cyclones and their implications for precipitation and wind speed extremes in simulations of the Maunder Minimum versus present day conditions, *Clim. Dynam.*, 28, 409–423, doi:10.1007/s00382-006-0188-7, 2007. 84

Raible, C. C., Della-Marta, P. M., Schwierz, C., Wernli, H., and Blender, R.: Northern hemisphere extratropical cyclones: A comparison of detection and tracking methods and different reanalyses, *Month. Weather Rev.*, 136, 880–897, doi:10.1175/2007MWR2143.1, 2008. 80

Ramstein, G., Kageyama, M., Guiot, J., Wu, H., Hly, C., Krinner, G., and Brewer, S.: How cold was Europe at the Last Glacial Maximum? A synthesis of the progress achieved since the first PMIP model-data comparison, *Clim. Past*, 3, 331–339, doi:10.5194/cp-3-331-2007, 2007. 66

Schilt, A., Baumgartner, M., Schwander, J., Buiron, D., Capron, E., Chappellaz, J., Loulergue, L., Schupbach, S., Spahni, R., Fischer, H., and Stocker, T. F.: Atmospheric nitrous oxide during the last 140 000 years, *Earth Planet. Sci. Lett.*, 300, 33–43, doi:10.1016/j.epsl.2010.09.027, 2010. 70, 91

Shin, S. I., Liu, Z., Otto-Bliesner, B., Brady, E. C., Kutzbach, J. E., and Harrison, S. P.: A simulation of the last glacial maximum climate using the NCAR-CCSM, *Clim. Dynam.*, 20, 127–151, doi:10.1007/s00382-002-0260-x, 2003. 66

Siddall, M., Rohling, E. J., Thompson, W. G., and Waelbroeck, C.: Marine Isotope Stage 3 Sea Level Fluctuations: Data Synthesis and New Outlook, *Rev. Geophys.*, 46, RG4003, doi:10.1029/2007RG000226, 2008. 65, 66, 70

Strandberg, G., Brandefelt, J., Kjellstrom, E., and Smith, B.: High-resolution regional simulation of last glacial maximum climate in Europe, *Tellus Series A-dynamic Meteorology and Oceanography*, 63, 107–125, doi:10.1111/j.1600-0870.2010.00485.x, 2011. 76, 79, 83

Toracinta, E. R., Oglesby, R. J., and Bromwich, D. H.: Atmospheric response to modified CLIMAP ocean boundary conditions during the Last Glacial Maximum, *J. Climate*, 17, 504–522, 2004. 84

Uppala, S. M., Kallberg, P. W., Simmons, A. J., Andrae, U., Bechtold, V. D., Fiorino, M., Gibson, J. K., Haseler, J., Hernandez, A., Kelly, G. A., Li, X., Onogi, K., Saarinen, S., Sokka, N., Allan, R. P., Andersson, E., Arpe, K., Balmaseda, M. A., Beljaars, A. C. M., Van De Berg, L., Bidlot, J., Bormann, N., Caires, S., Chevallier, F., Dethof, A., Dragosavac, M., Fisher, M., Fuentes, M., Hagemann, S., Holm, E., Hoskins, B. J., Isaksen, L., Janssen, P. A. E. M.,

**Sensitivity to glacial boundary conditions**

D. Hofer et al.

- Jenne, R., McNally, A. P., Mahfouf, J. F., Morcrette, J. J., Rayner, N. A., Saunders, R. W., Simon, P., Sterl, A., Trenberth, K. E., Untch, A., Vasiljevic, D., Viterbo, P., and Woollen, J.: The ERA-40 re-analysis, *Q. J. Roy. Meteorol. Soc.*, 131, 2961–3012, doi:10.1256/qj.04.176, 2005. 68, 71, 72, 82
- 5 Waelbroeck, C., Paul, A., Kucera, M., Rosell-Melee, A., Weinelt, M., Schneider, R., Mix, A. C., Abelmann, A., Armand, L., Bard, E., Barker, S., Barrows, T. T., Benway, H., Cacho, I., Chen, M. T., Cortijo, E., Crosta, X., de Vernal, A., Dokken, T., Duprat, J., Elderfield, H., Eynaud, F., Gersonde, R., Hayes, A., Henry, M., Hillaire-Marcel, C., Huang, C. C., Jansen, E., Juggins, S., Kallel, N., Kiefer, T., Kienast, M., Labeyrie, L., Leclaire, H., Londeix, L., Mangin, S.,
- 10 Matthiessen, J., Marret, F., Meland, M., Morey, A. E., Mulitza, S., Pflaumann, U., Pisias, N. G., Radi, T., Rochon, A., Rohling, E. J., Saffi, L., Schafer-Neth, C., Solignac, S., Spero, H., Tachikawa, K., and Turon, J. L.: Constraints on the magnitude and patterns of ocean cooling at the Last Glacial Maximum, *Nature Geosci.*, 2, 127–132, doi:10.1038/NGEO411, 2009. 65
- 15 Wu, H. B., Guiot, J. L., Brewer, S., and Guo, Z. T.: Climatic changes in Eurasia and Africa at the last glacial maximum and mid-Holocene: reconstruction from pollen data using inverse vegetation modelling, *Clim. Dynam.*, 29, 211–229, doi:10.1007/s00382-007-0231-3, 2007. 65, 66, 74, 75, 83, 95

Title Page

Abstract

Introduction

Conclusions

References

Tables

Figures

◀

▶

◀

▶

Back

Close

Full Screen / Esc

Printer-friendly Version

Interactive Discussion



## Sensitivity to glacial boundary conditions

D. Hofer et al.

**Table 1.** Overview of the simulations for the two model versions and the ice sheet topographies applied in CCSM4. The monthly mean SST and sea ice data of the five CCSM3 simulations are used as inputs for the corresponding CCSM4 experiments. The MW simulation for CCSM3 uses the same topography as the LGM one and its SST and sea ice fields serve as input in all the CCSM4's MW experiments – which differ only in their ice sheet topographies (see also Fig. 1 and text). The values for the ice sheet heights indicate how much of Peltier's LGM-PD topography changes are applied for the Fennoscandian, the Laurentide and all other (mainly Greenland and Antarctica) ice sheets.

Description	CCSM3	CCSM4	Ice sheet heights		
	Label	Label	Fennoscandian	Laurentide	Others
Transient 1971–2000 AD simulation	–	PDTR	0 %	0 %	0 %
1990 AD simulation	PD3 <sup>a</sup>	PD	0 %	0 %	0 %
1850 AD simulation	PI3 <sup>b</sup>	PI	0 %	0 %	0 %
–21 ka simulations	LGM13 <sup>c</sup>	LGM1	100 %	100 %	100 %
	LGM23 <sup>d</sup>	LGM2	100 %	100 %	100 %
–65 ka simulations	MW3 <sup>e</sup>	MWLGM	100 %	100 %	100 %
		MWLIN	67 %	67 %	67 %
		MWEU	33 %	76 %	76 %
		MWUS	100 %	46 %	100 %
		MWNS	100 % <sup>f</sup>	46 %	100 %

<sup>a</sup> year 901–930 from the NCAR's present-day simulation (Otto-Bliesner et al., 2006b)

<sup>b</sup> year 663–692 from the NCAR's preindustrial simulation (Otto-Bliesner et al., 2006b)

<sup>c</sup> started from year 250 of the NCAR's LGM simulation (Otto-Bliesner et al., 2006a)

<sup>d</sup> year 1766–1795 of the LGM simulation of Brandefelt and Otto-Bliesner (2009)

<sup>e</sup> started from year 250 of the NCAR's LGM simulation (Otto-Bliesner et al., 2006a) and run into equilibrium for 300 yr

<sup>f</sup> except for the North Sea, which is at 0 %

Title Page

Abstract

Introduction

Conclusions

References

Tables

Figures

◀

▶

◀

▶

Back

Close

Full Screen / Esc

Printer-friendly Version

Interactive Discussion





## Sensitivity to glacial boundary conditions

D. Hofer et al.

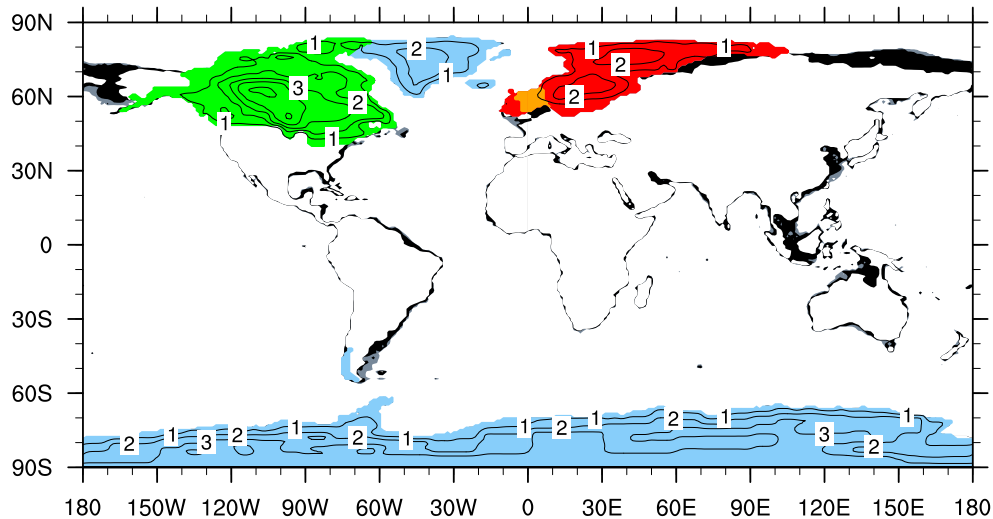


**Fig. 1.** LGM ice sheet extent (all colored areas) and thickness (contours, interval 1 km), and additional land areas in MW (black) and LGM (black and gray). The different colors indicate the regions of the strongest reduction of the ice sheet height in the MW simulations compared with the LGM one (see also text): red and orange for MWEU, green for MWUS, and green and orange for MWNS. The coastlines and ice sheets for LGM are based on ICE-5G (Peltier, 2004). The shift of the coastlines (shown as the boundary of 50% landfraction) corresponds to a sea-level change of 80 m (MW) and 120 m (LGM) with respect to today.

Title Page

Abstract

Introduction

Conclusions

References

Tables

Figures

◀

▶

◀

▶

Back

Close

Full Screen / Esc

Printer-friendly Version

Interactive Discussion



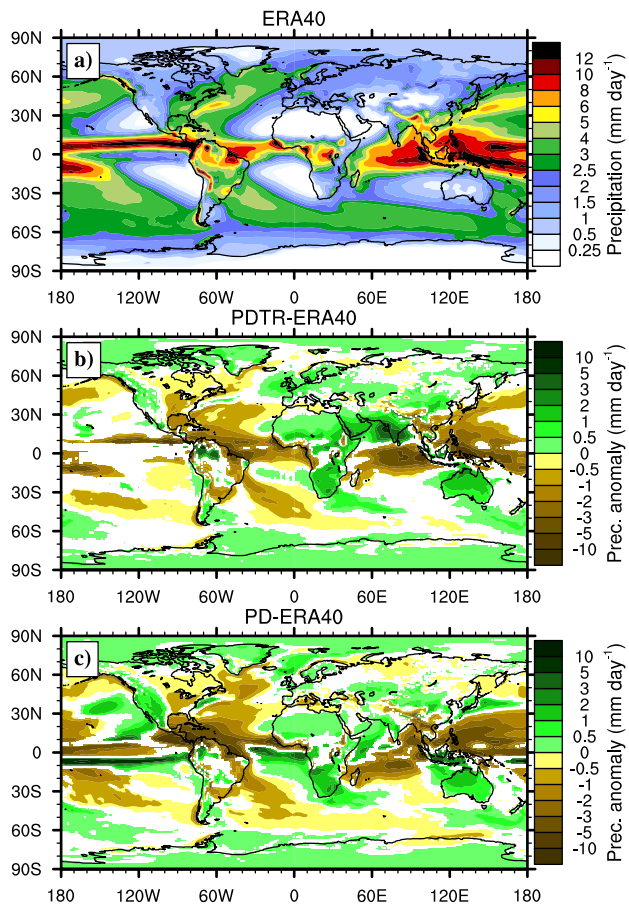


**Fig. 2.** (a) Mean precipitation for ERA40 (averaged from 1971–2000) and the anomalies of (b) PDTR and (c) PD. In the anomaly plots only values that are statistically significant at the 5% level based on the two-sided Student's  $t$  test are colored.

## Sensitivity to glacial boundary conditions

D. Hofer et al.

Title Page

Abstract

Introduction

Conclusions

References

Tables

Figures

◀

▶

◀

▶

Back

Close

Full Screen / Esc

Printer-friendly Version

Interactive Discussion



## Sensitivity to glacial boundary conditions

D. Hofer et al.

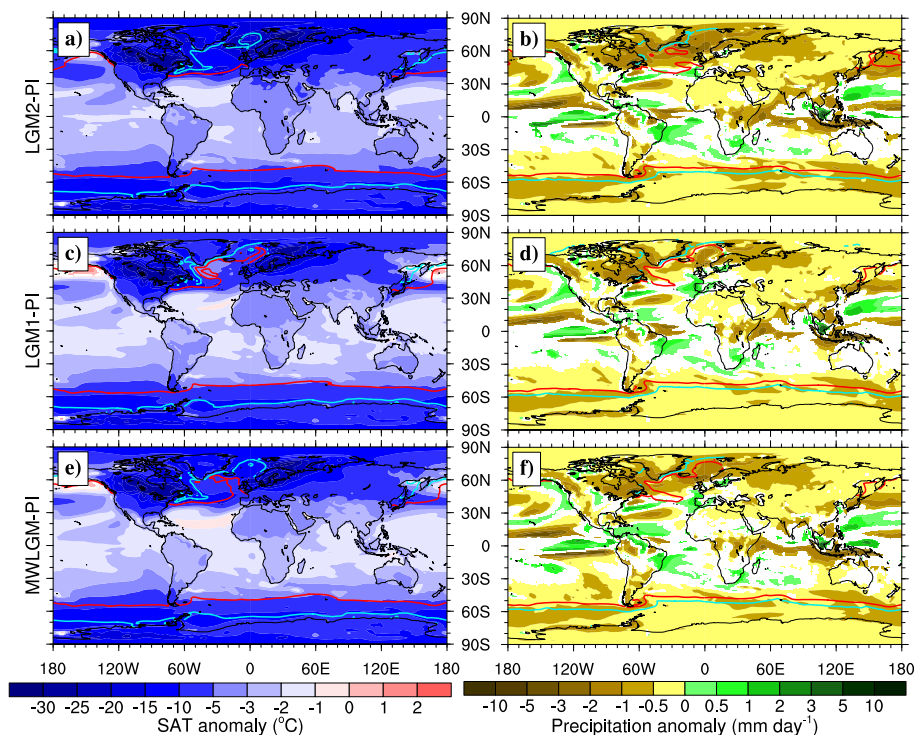


**Fig. 3.** SAT and precipitation anomalies with respect to PI for LGM2 (**a** and **b**), LGM1 (**c** and **d**), and MWLGM (**e** and **f**). Only values that are statistically significant at the 5% level based on the two-sided Student's  $t$  test are colored. The contour indicates the DJF (left) and JJA (right) sea ice extent (cyan and red lines for 90% and 10% seasonal mean ice fraction, respectively).

Title Page

Abstract

Introduction

Conclusions

References

Tables

Figures

◀

▶

◀

▶

Back

Close

Full Screen / Esc

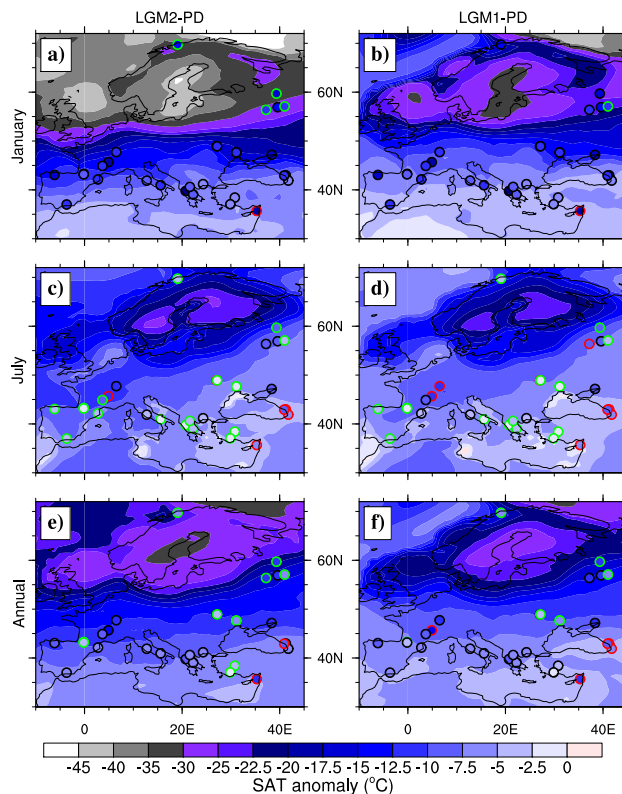
Printer-friendly Version

Interactive Discussion



## Sensitivity to glacial boundary conditions

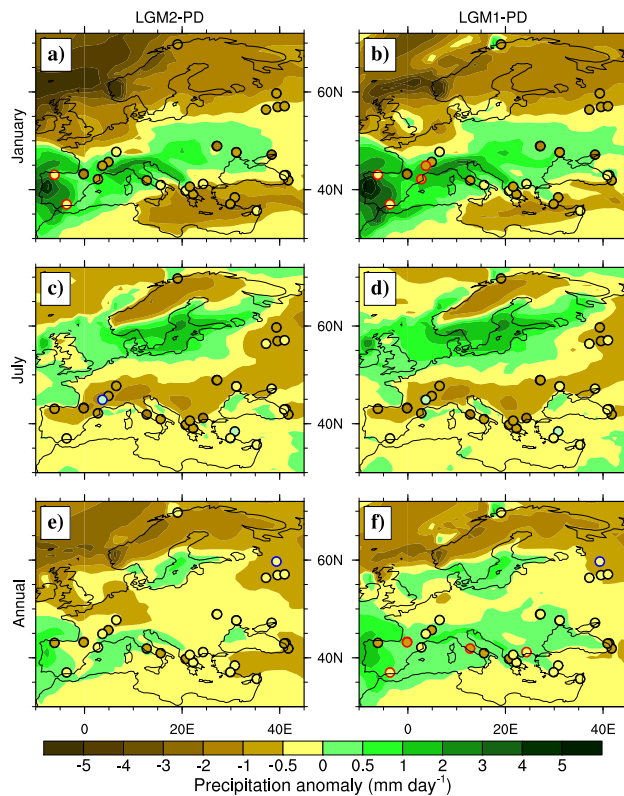
D. Hofer et al.



**Fig. 4.** SAT anomalies with respect to PD for LGM2 (left) and LGM1 (right) for the coldest month (January, **a** and **b**), the warmest month (July, **c** and **d**), and the annual mean (**e** and **f**). The colored circles are estimated temperature anomalies based on proxy data (Wu et al., 2007) with a red (green) border indicating significantly stronger (weaker) negative anomalies than at the closest grid cell of the model (outside the 90% confidence interval of Wu et al., 2007).

**Sensitivity to glacial boundary conditions**

D. Hofer et al.

**Fig. 5.** As Fig. 4, but for precipitation.

Title Page

Abstract

Introduction

Conclusions

References

Tables

Figures

◀

▶

◀

▶

Back

Close

Full Screen / Esc

Printer-friendly Version

Interactive Discussion



## Sensitivity to glacial boundary conditions

D. Hofer et al.

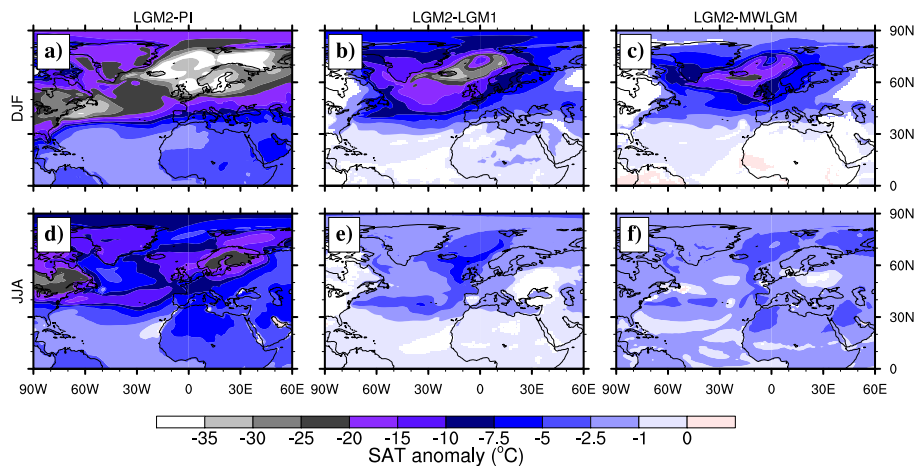


**Fig. 6.** Winter (DJF, top) and summer (JJA, bottom) SAT anomalies of LGM2 with respect to PI (a and d), and of LGM1 (b and e) and MWLGM (c and f) with respect to LGM2. Only values that are statistically significant at the 5% level based on the two-sided Student's  $t$  test are colored.

[Title Page](#)[Abstract](#)[Introduction](#)[Conclusions](#)[References](#)[Tables](#)[Figures](#)[◀](#)[▶](#)[◀](#)[▶](#)[Back](#)[Close](#)[Full Screen / Esc](#)[Printer-friendly Version](#)[Interactive Discussion](#)

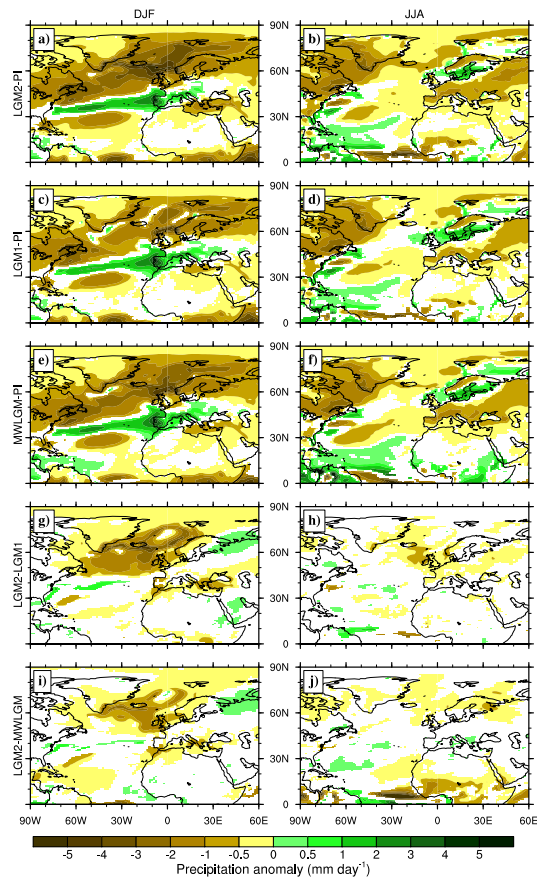


**Fig. 7.** Winter (DJF, left) and summer (JJA, right) precipitation anomalies for LGM2 (**a** and **b**), LGM1 (**c** and **d**) and MWLGM (**e** and **f**) with respect to PI, and additionally the anomalies LGM2-LGM1 (**g** and **h**) and LGM2-MWLGM (**i** and **j**). Only the values that are statistically significant at the 5 % level based on the two-sided Student's *t* test are colored.

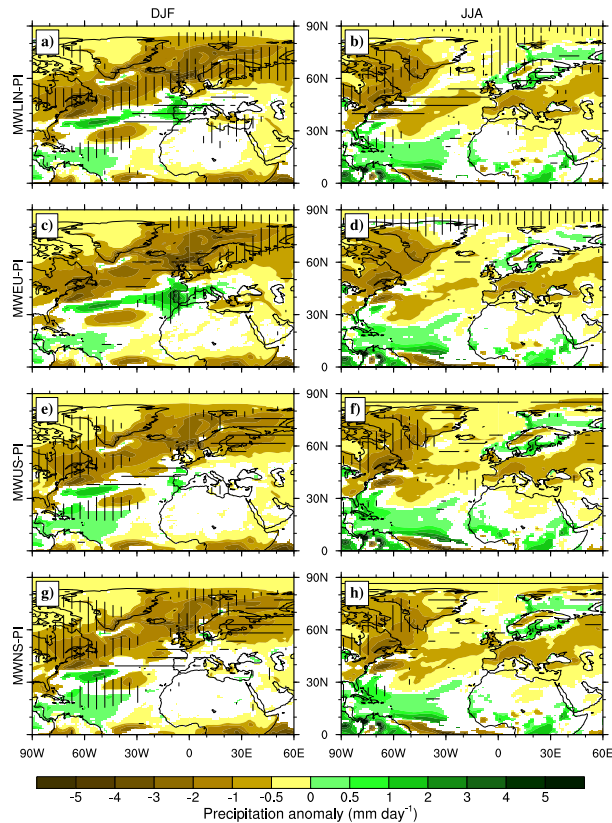


**Fig. 8.** Winter (DJF, left) and summer (JJA, right) precipitation anomalies with respect to PI for MWLIN (a and b), MWEU (c and d), MWUS (e and f), and MWNS (g and h). Only values that are statistically significant at the 5% level based on the two-sided Student's  $t$  test are colored. For MWLIN vertical (horizontal) bars indicate regions where MWLGM is significantly (also at the 5% level) wetter (drier). In the other three cases the meaning of the bars is the same, but with respect to MWLIN.

## Sensitivity to glacial boundary conditions

D. Hofer et al.

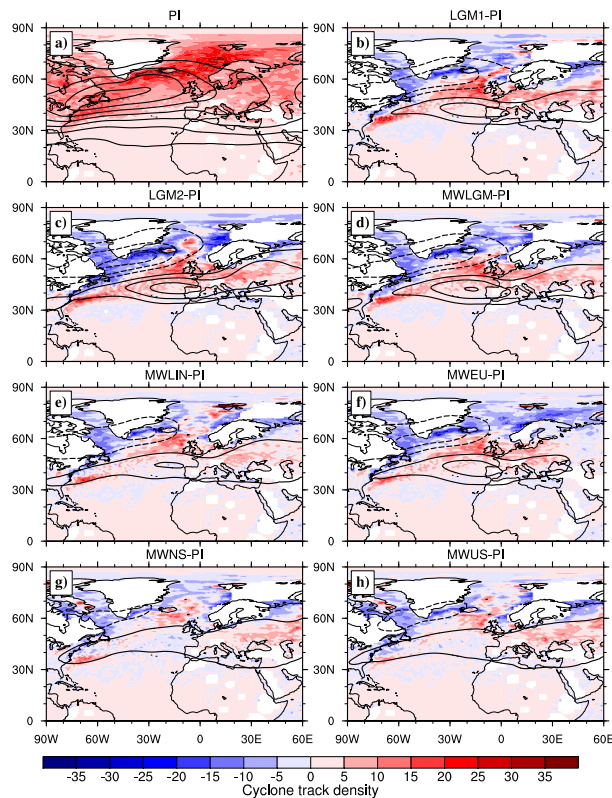


**Fig. 9.** Synoptic activity in winter (DJF) using two different measures, namely cyclone track density (colors, only values where the altitude is below 1000 m) and band-pass filtered (2.5 to 6 days) standard deviation of the 500 hPa geopotential height (contours). The mean value for PI are shown in (a) while in (b)–(h) the anomalies of the different glacial simulations with respect to PI are presented. The contour interval is every 10 gpm, negative contours are dashed and the zero contour line is omitted.

Title Page

Abstract

Introduction

Conclusions

References

Tables

Figures

◀

▶

◀

▶

Back

Close

Full Screen / Esc

Printer-friendly Version

Interactive Discussion



Sensitivity to glacial  
boundary conditions

D. Hofer et al.

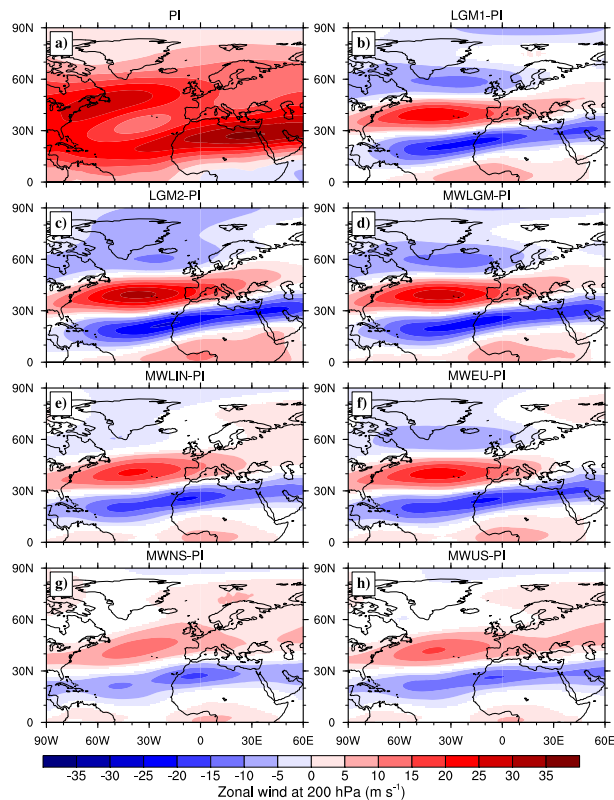


**Fig. 10.** Zonal wind at 200 hPa for DJF. The mean value for PI are shown in (a) while in (b)–(h) the anomalies of the different glacial simulations with respect to PI are presented. For the anomalies only values that are statistically significant at the 5 % level based on the two-sided Student's  $t$  test are colored.

Title Page

Abstract

Introduction

Conclusions

References

Tables

Figures

◀

▶

◀

▶

Back

Close

Full Screen / Esc

Printer-friendly Version

Interactive Discussion

